Significance of hub genes and immune cell infiltration identified by bioinformatics analysis in pelvic organ prolapse

Ying Zhao, Zhijun Xia, Te Lin and Yitong Yin

Department of Obstetrics and Gynecology, Pelvic Floor Disease Diagnosis and Treatment Center, Shengjing Hospital of China Medical University, Shenyang, China

ABSTRACT

Objective: Pelvic organ prolapse (POP) refers to the decline of pelvic organ position and dysfunction caused by weak pelvic floor support. The aim of the present study was to screen the hub genes and immune cell infiltration related to POP disease.
Methods: Microarray data of 34 POP tissues in the GSE12852 gene expression dataset were used as research objects. Weighted gene co-expression network analysis (WGCNA) was performed to elucidate the hub module and hub genes related to POP occurrence. Gene function annotation was performed using the DAVID tool. Differential analysis based on the GSE12852 dataset was carried out to explore the expression of the selected hub genes in POP and non-POP tissues, and RT-qPCR was used to validate the results. The differential immune cell infiltration between POP and non-POP tissues was investigated using the CIBERSORT algorithm.
Results: WGCNA revealed the module that possessed the highest correlation with POP occurrence. Functional annotation indicated that the genes in this module were mainly involved in immunity. *ZNF331*, *THBS1*, *IFRD1*, *FLJ20533*, *CXCR4*, *GEM*, *SOD2*, and *SAT* were identified as the hub genes. Differential analysis and RT-qPCR demonstrated that the selected hub genes were overexpressed in POP tissues as compared with non-POP tissues. The CIBERSORT algorithm was employed to evaluate the infiltration of 22 immune cell types in POP tissues and non-POP tissues. We found greater infiltration of activated mast cells and neutrophils in POP tissues than non-POP tissues, while the infiltration of resting mast cells was lower in POP tissues. Moreover, we investigated the relationship between the type of immune cell infiltration and hub genes by Pearson correlation analysis. The results indicate that activated mast cells and neutrophils had a positive correlation with the hub genes, while resting mast cells had a negative correlation with the hub genes.
Conclusions: Our research identified eight hub genes and the infiltration of three types of immune cells related to POP occurrence. These hub genes may participate in the pathogenesis of POP through the immune system, giving them a certain diagnostic and therapeutic value.

Subjects Bioinformatics, Allergy and Clinical Immunology, Gynecology and Obstetrics, Internal Medicine, Women's Health
Keywords Pelvic organ prolapse, WGCNA, CIBERSORT, Immune cells infiltration, GEO database

Submitted 12 March 2020
Accepted 30 July 2020
Published 18 August 2020

Corresponding author
Zhijun Xia, xiazj@sj-hospital.org

Academic editor
Dezső Módos

Additional Information and Declarations can be found on page 15

DOI **10.7717/peerj.9773**

Copyright
2020 Zhao et al.

Distributed under
Creative Commons CC-BY 4.0

OPEN ACCESS

INTRODUCTION

Pelvic organ prolapse (POP) is caused by dysfunction of the pelvic floor supporting structures and affects the quality of life of many women (*Nygaard et al., 2014*). The prevalence of POP is expected to reach 46% by 2050 (*Wu et al., 2009*). Currently, only approximately 20% of women have POP surgery during their lifetime (*Haya et al., 2018*); however, the reoperation rate is high (*Friedman, Eslick & Dietz, 2018*), which causes a huge economic burden. POP is a complex, multifaceted disease resulting from the interaction between environmental and genetic factors. Pregnancy, vaginal pull-up, time of delivery, age, and obesity have been identified as risk factors (*Hendrix et al., 2002*); nevertheless, the molecular mechanism of POP remains unclear, and there is a lack of suitable prevention and treatment measures in clinical practice. Therefore, it is imperative to explore the molecular mechanism of POP occurrence for the benefit for both women and society.

Owing to the development of gene chips and new generation sequencing technology, bioinformatics analysis plays an increasingly important role in biomedical research. Weighted gene co-expression network analysis (WGCNA) can identify gene module characteristics and hub genes to connect the gene modules and sample characteristics (*Wang et al., 2020b*). The CIBERSORT algorithm can be employed to evaluate immune cell infiltration in tissues based on gene expression datasets. Recently, abundant researches have used this algorithm to explore the function of immune cells in diseases (*Lin et al., 2020*), breast ductal and lobular carcinoma (*Zhang et al., 2019*), osteoarthritis (*Cai et al., 2020*), and high-grade serous ovarian cancer (*Liu et al., 2020*). Our study found hub genes and immune cells highly related to POP occurrence by analyzing POP expression spectrum data in public databases using WGCNA and the CIBERSORT algorithm, providing novel ideas and methods for the treatment of POP. Finally, the differential immune cells was investigated between POP and non-POP tissues.

MATERIALS AND METHODS

Obtaining the training and validation POP datasets

The workflow diagram is presented in Fig. 1. The training dataset was obtained from the Gene Expression Omnibus database (GEO, https://www.ncbi.nlm.nih.gov/) in NCBI based on the keywords "pelvic organ prolapse" and "gene expression profiles" and "*Homo sapiens*" (*Brizzolara, Killeen & Urschitz, 2009*). In addition, we selected a dataset with a sample size greater than 30, which is the minimum sample size required to construct a WGCNA network (POP > 15, non-POP > 15); the GSE12852 dataset, containing 16 POP and 18 non-POP patients, was the only dataset to meet this condition. The gene expression profiles and corresponding clinical information including age, menopausal status, race, and prolapse stage were acquired from the GSE12852 dataset. Subsequently, log-scale robust multi-array analysis was used to perform background correction and normalization of the datasets. A total of 12 POP patients enrolled at the Shengjing Hospital of China Medical University from 2017 to 2018 were selected as the validation dataset. The Ethics Committee of Shengjing Hospital of China Medical University approved the

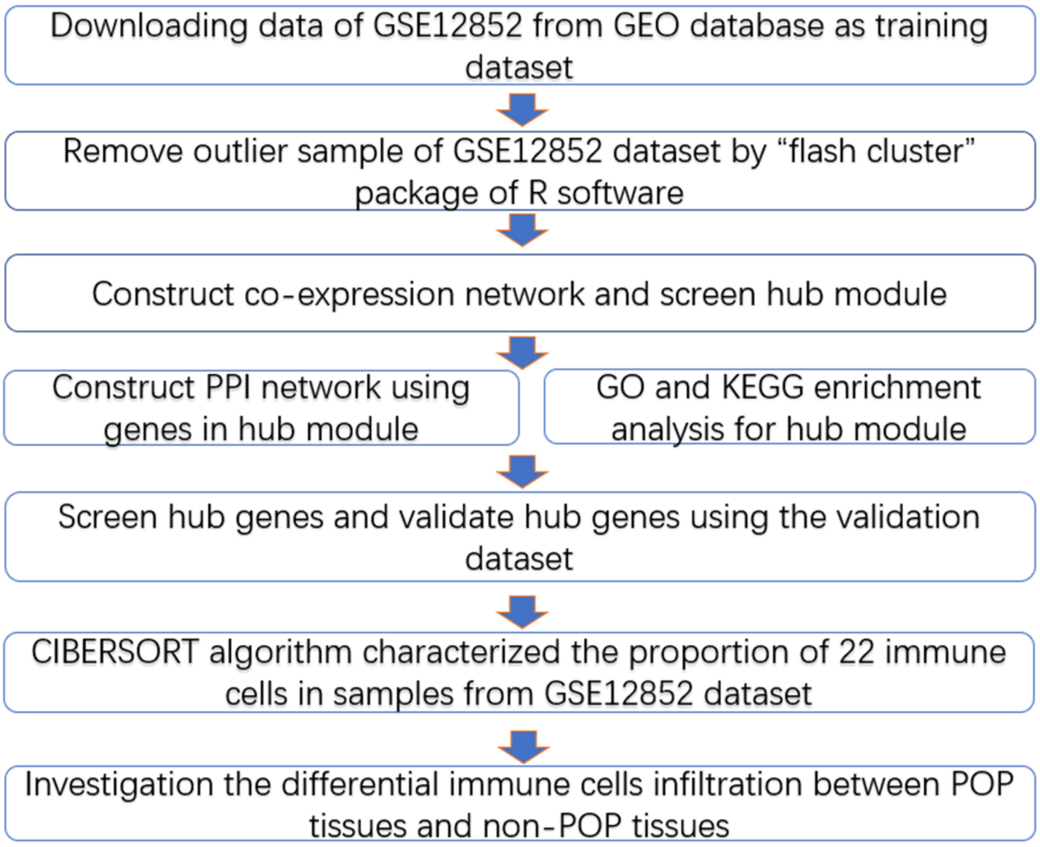

Figure 1 Workflow diagram. Data collection, analysis and validation.
Full-size DOI: 10.7717/peerj.9773/fig-1

study protocol in accordance with the guidelines of the Declaration of Helsinki (No. 2018Ps68K), and our study was exempt from consent. Prolapse tissues were selected as the experimental group and non-prolapse tissues were selected as the control group. All patients were married, without estrogen-related disorders, and had received no hormone treatment within the previous 3 months. Basic information of the patients in the validation dataset is presented in Table S1.

Co-expression network construction based on the training dataset

We used the "WGCNA" package of the R software to establish the network based on the 34 samples in the training dataset according to a previously described method (*Chen et al., 2018b*; *Zhou et al., 2018*). Firstly, POP and normal samples were analyzed using the "flash cluster" package of the R software to remove outlier samples. The correlation matrix of gene co-expression consists of the correlation coefficient between two genes. The average linkage matrix and Pearson correlation method were performed to construct the correlation matrix between genes. Subsequently, the formula $amn = |cmn|^{\beta}$ was used to convert the correlation matrix to the adjacency matrix (*amn* represents the correlation coefficient between gene *m* and gene *n*; *cmn* represents the connection coefficient between gene *m* and gene *n*; and β is a soft threshold that can strengthen strong links between genes

and weaken weak links). Finally, we converted the adjacency matrix to the topological overlap matrix based on an appropriate soft threshold, and placed the similar genes into the same module.

Identification of hub gene modules and genes

Similar genes were placed into the same module based on the WGCNA co-expression network. The main purpose of our research was to combine clinical information (POP or non-POP samples) with gene modules to analyze gene significance (GS) and modular membership (MM). MM means the correlation between gene expression profile level and module eigengenes (ME). ME are considered the correlation between modules and clinical information. GS represents the degree of correlation between gene expression profiles and clinical information. The average value of all gene GS in the module represents the module significance (MS). We defined the correlation between gene and disease as GS, and obtained the correlation between this module and disease as MS. The hub genes characterized by a high MM and a high GS are described as having the closest relationship with disease. In our research, the module with the highest MS was selected as the hub module. The genes in the hub module with $|MM| > 0.8$ and $|GS| > 0.47$ were considered hub genes.

Functional enrichment analysis

We used the online GO enrichment analysis and KEGG pathway analysis tools on the DAVID website to annotate the genes in the module identified by WGCNA, and attempted to elucidate the enrichment pathway and functions of the target genes. The Human Genome U133 Plus 2 Array was used as the background data (The FDR < 0.01).

Immune cell infiltration in POP tissues

CIBERSORT is an algorithm to characterize the proportion of 22 immune cells (Table S2) in tissues using 547 barcode gene expression values. The CIBERSORT algorithm was employed to elucidate the proportion of 22 immune cells in POP tissues. The samples with p value < 0.05 were significant (*Chen et al., 2018a*). Pearson correlation analysis was implemented to obtain the related coefficient between the 22 immune cells. Then, we investigated the differential immune cell infiltration between POP and non-POP tissues. Finally, we calculated the related coefficient between infiltration of different immune cells and hub genes by Pearson correlation analysis.

RNA extraction and quantitative real-time PCR based on the validation dataset

TRIzol® (one mL) was used to isolate total RNA from POP tissues (200 mg) in the validation dataset, and reverse transcriptase from the avian myeloblastoma virus and random primers were used to create complementary DNA (cDNA) according to the instructions from TAKARA. SYBR Premix Ex Taq II (Takara, Shiga, Japan) was used to amplify the cDNA. According to the samples from three independent experiments, the $2^{-\Delta\Delta CT}$ value was used to analyze the data. Primers for the genes are displayed in Table S3.

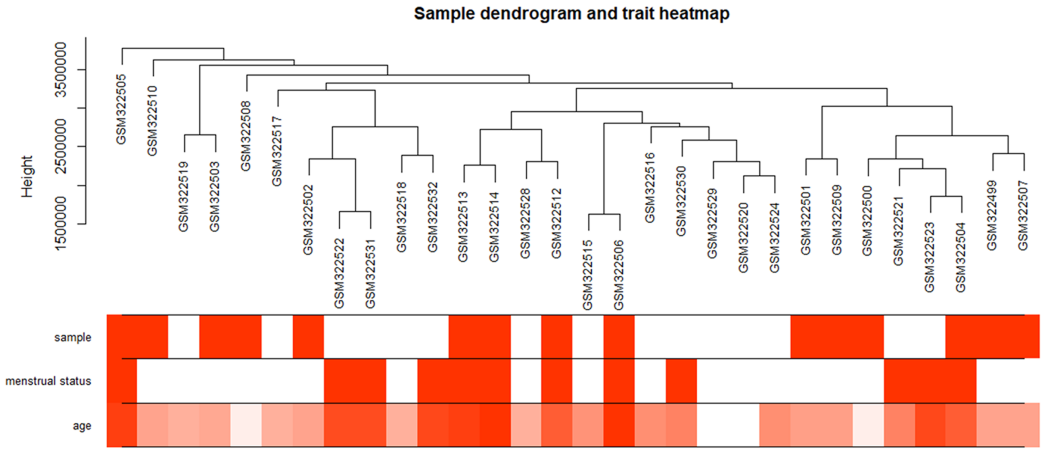

Figure 2 Clustering dendrogram of 34 POP samples in GSE12852. POP samples were assigned as 1; non-POP samples were assigned as 0. Pre-menopause status samples were assigned as 0; menopause status samples were assigned as 1. Red color intensity is proportional to POP samples, pre-menopause status, and higher age. Full-size DOI: 10.7717/peerj.9773/fig-2

Statistical analysis

The GraphPad Prism 7.0 and R 3.6.1 software were used for statistical analysis and image generation. A *t*-test was employed to analyze the differences between two groups. The $p < 0.05$ was statistically significant.

RESULTS

Construction of WGCNA and identification of hub modules

The "flash cluster" software package in R was used to cluster the 34 samples in the GSE12852 dataset to remove the outlier samples; four outlier samples were removed (Fig. 2). There were few differences among the remaining samples, which is conducive to the accuracy of the results. The correlation matrix between genes was calculated according to the average linkage matrix and Pearson correlation method. The formula $amn = |cmn|^{\beta}$ ($\beta = 7$) was used to transform the correlation matrix into the adjacency matrix. In order to better construct a scale-free network distribution, the "picks of threshold" function of "WGCNA" package calculated the value of parameter β. In POP and non-POP samples, 1–20 thresholds were selected and the correlation coefficient, mean connectivity, and average correlation degree between log (k) and log (P (k)) were calculated for each threshold. At this time, the average network connectivity corresponding to the threshold is close to zero, indicating that the network connectivity is very low, which is similar to the scale-free network (Fig. 3). According to the corresponding steps of WGCNA, the gene network was built after the hierarchical clustering tree. In this experiment, the dynamic pruning tree method merged with similar genes into one gene module. The minimum number of genes in a module was 30, and 11 modules were obtained (Fig. 4A). According to the thermogram of correlation between modules and clinical information, the highest correlation existed in the blue module and sample type, with a correlation coefficient of 0.47 (Fig. 4B; $p = 0.009$). Therefore, the blue module was

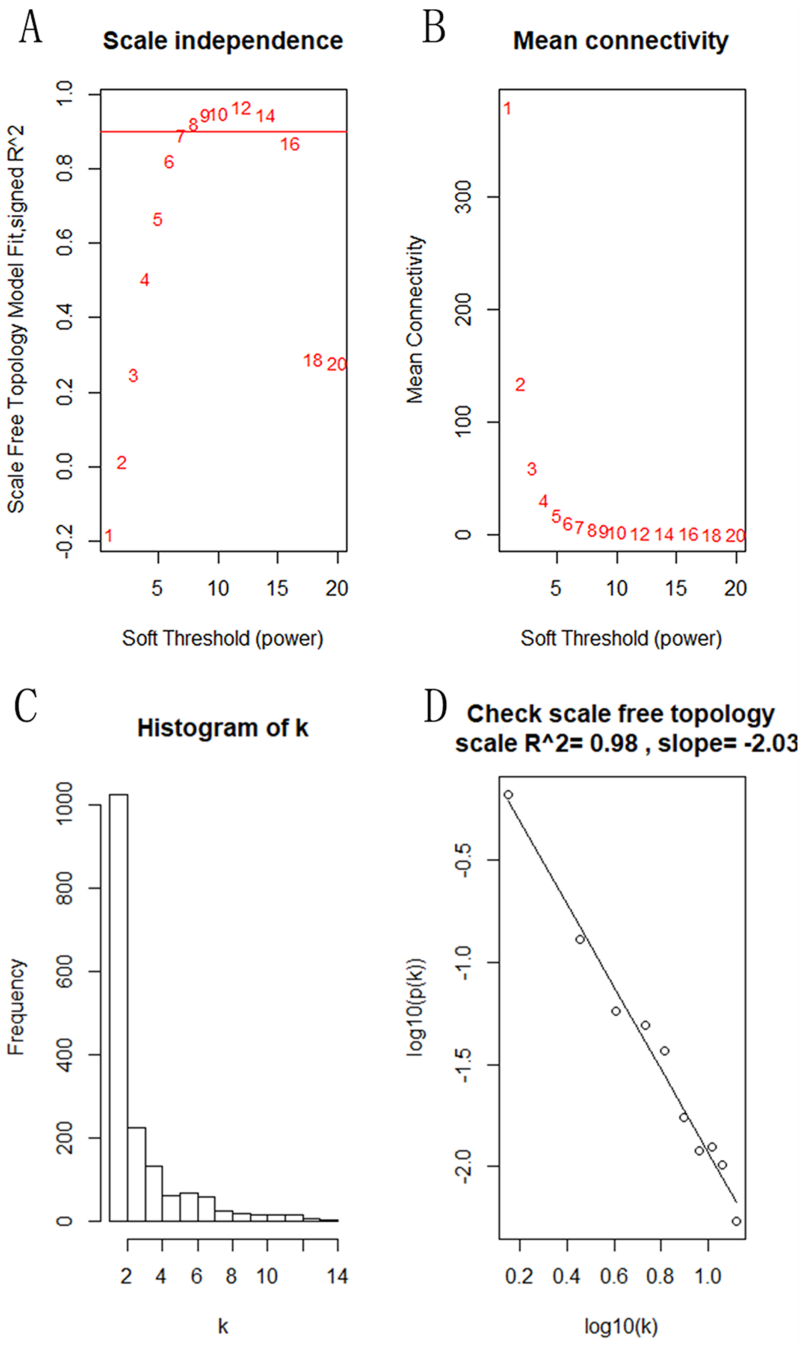

Figure 3 Identification of the soft threshold in the scale-free network. (A) Different soft-threshold and corresponding scale free topology model. (B) Different soft-thresholding powers and corresponding mean connectivity. (C) The distribution of the connectedness by histogram. (D) Inspection of the scale free topology. Full-size DOI: 10.7717/peerj.9773/fig-3

considered the most study-worthy. Protein–protein interactions (PPIs) are widely involved in the process of vital movement. http://omnipathdb.org/ was used to construct the PPI network for genes in the blue module (Fig. 5) (*Türei, Korcsmáros & Saez-Rodriguez, 2016*).

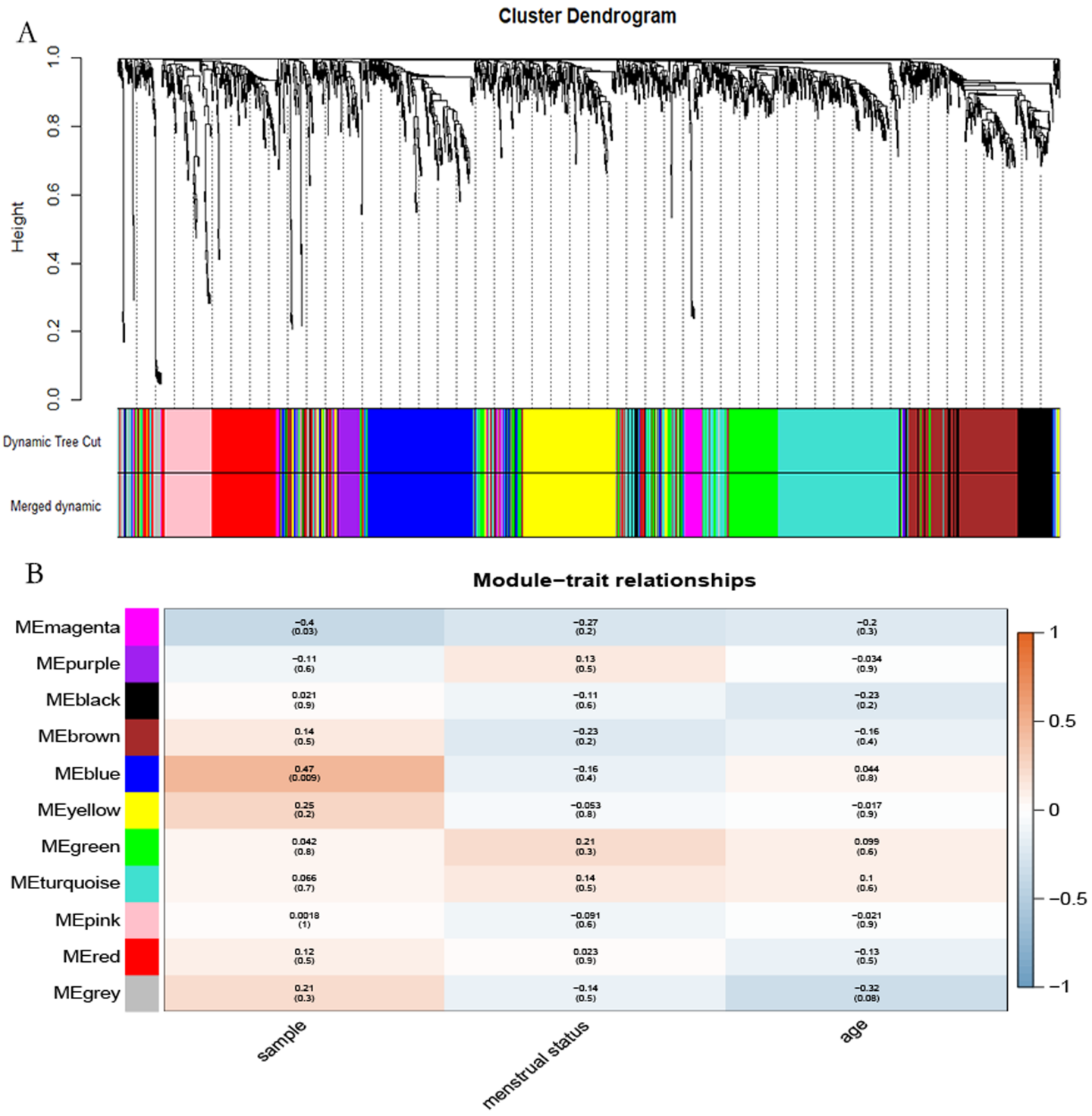

Figure 4 **Identification of the hub module.** (A) Dendrogram showed the genes with similar function classed into the same module according to the dissimilarity measure. (B) Heatmap revealed the correlation between modular eigengenes (ME) and clinical information of POP.

Full-size DOI: 10.7717/peerj.9773/fig-4

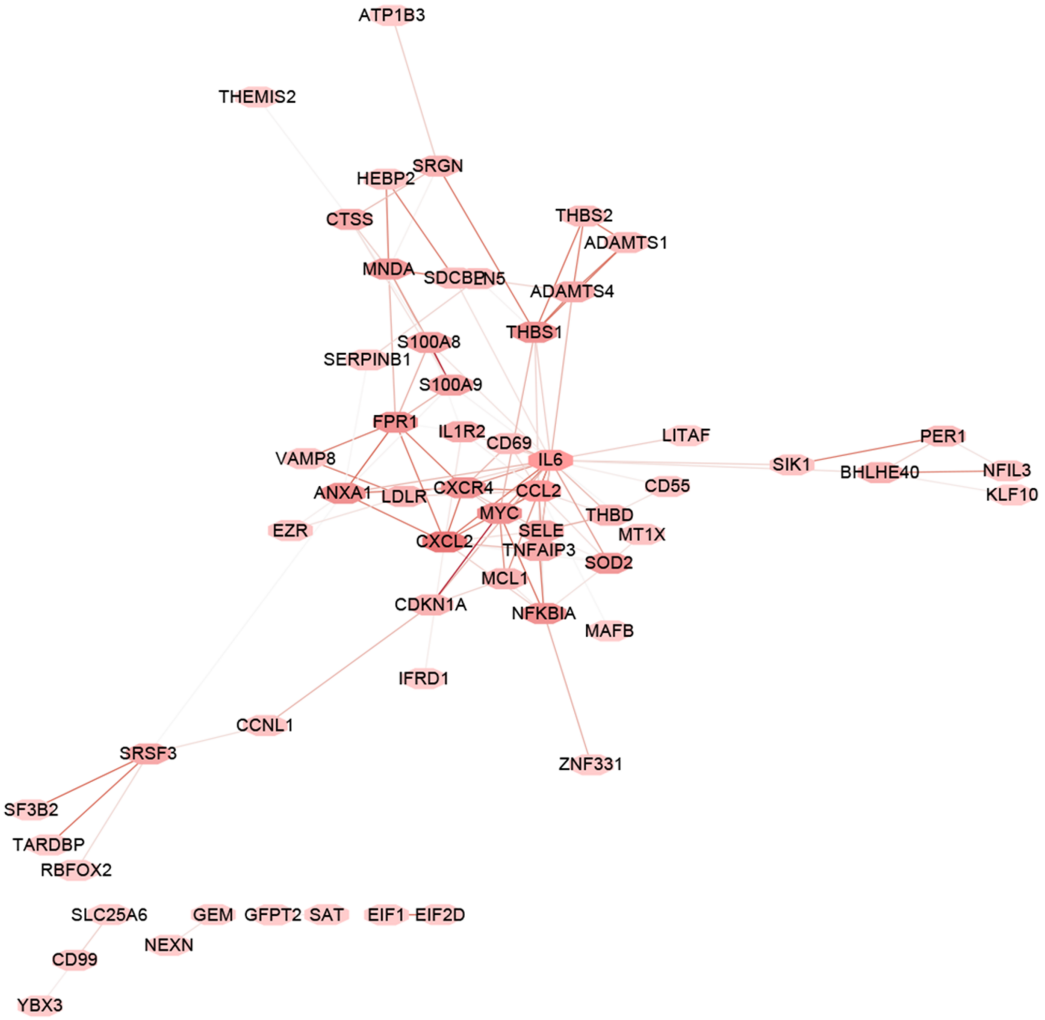

Figure 5 PPI network analysis. PPI network analysis of the genes in the blue module based on the OmniPath online database. Nodes represent the hub genes in the blue module identified by WGCNA. Lines represent interactions between hub genes. Full-size DOI: 10.7717/peerj.9773/fig-5

Functional enrichment analysis

To further study the biological function of the genes in the blue module, GO and KEGG enrichment analyses were used. GO enrichment analysis showed that these genes mainly participated in the immune regulation (Fig. 6A; Table S4). KEGG enrichment analysis identified that these genes participated in the regulation of immune-related pathways, such as the IL-17 and TNF signaling pathways (Fig. 6B; Table S5).

Identification of the hub genes

According to the screening criteria |MM| > 0.8 and |GS| > 0.47, eight genes (*ZNF331*, *THBS1*, *TMEM70*, *CXCR4*, *GEM*, *SOD2*, and *SAT*) were identified in the blue module as hub genes (Fig. 7A). We found that the hub genes were highly expressed in POP tissues as compared with non-POP tissues by differential analysis based on the GSE12852 dataset (Fig. 7B). From the heatmap, it can be seen that hub genes are overexpressed in POP

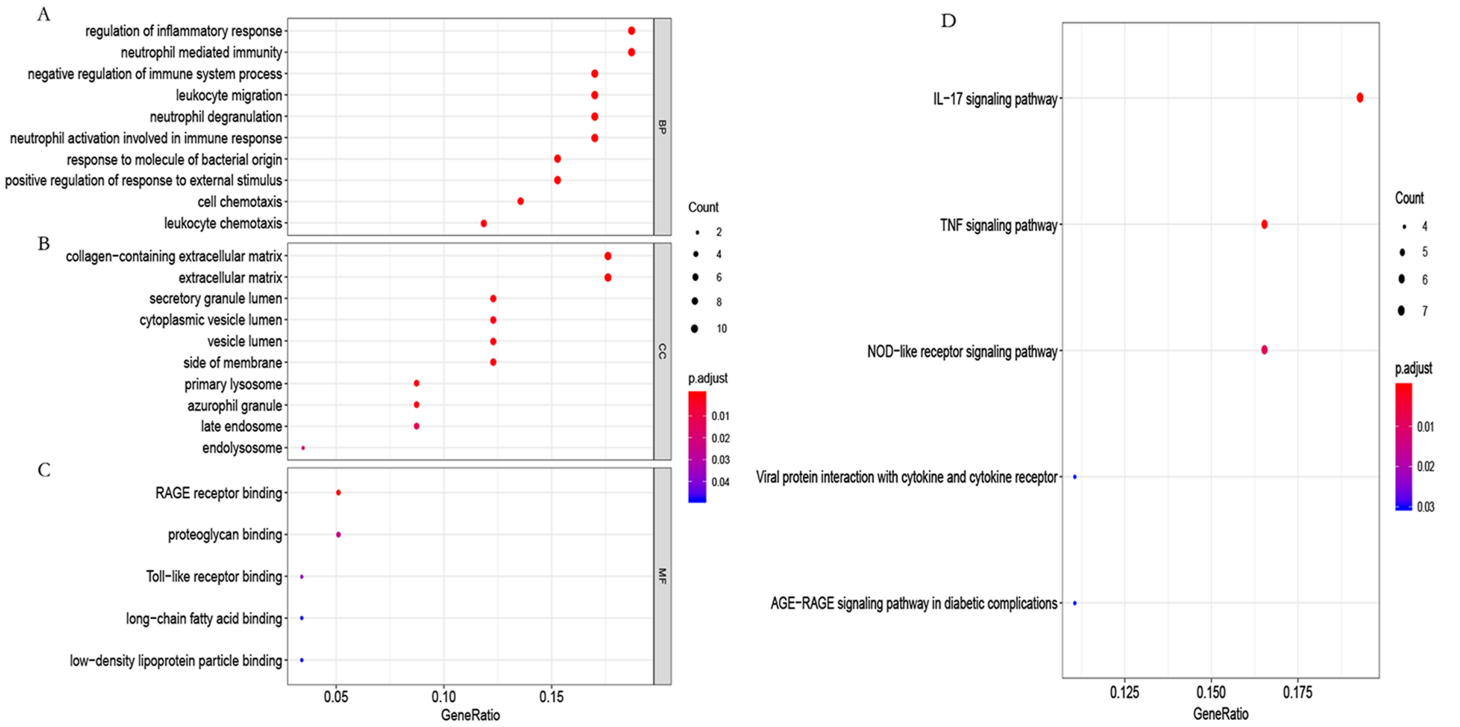

Figure 6 GO functional and KEGG pathway enrichment analysis. (A) Biological process (BP), (B) cellular component (CC) and (C) molecular function (MF) of GO analyzed by the "org.Hs.eg.db" package in the R software. (D) KEGG pathway enrichment analysis using the "org.Hs.eg.db" package in the R software.
Full-size DOI: 10.7717/peerj.9773/fig-6

tissues (Fig. 7C). In addition, the correlation coefficient between the hub genes was calculated, which showed that there was a strong co-expression relationship between these genes (Fig. 7D).

Validation of the hub genes

To verify the accuracy of the prediction results, RT-qPCR was used to detect the expression of the hub genes in 12 pairs of POP and non-POP tissues. The results show that the hub genes were overexpressed in POP tissues, which is consistent with the prediction results (Figs. 8A–8H).

Immune cell infiltration analysis

The CIBERSORT algorithm was employed to select samples with a output $p < 0.05$. A total of 12 samples including four non-POP and eight POP tissues were obtained. A bar plot was generated to show the proportion of 22 immune cells in the 12 samples (Fig. 9A). We found that macrophages account for the largest proportion among the immune cells in the samples. Figure 9B indicates that M1 macrophages had the strongest positive correlation with resting mast cells (correlation coefficient, 0.58), whereas resting mast cells had the strongest negative correlation with activated mast cells (correlation coefficient, 0.83). We found a higher infiltration of activated mast cells and neutrophils in POP tissues than in non-POP tissues, while the infiltration of resting mast cells was lower in POP tissues (Fig. 10; $p < 0.05$). Finally, Pearson correlation analysis was used to calculate the

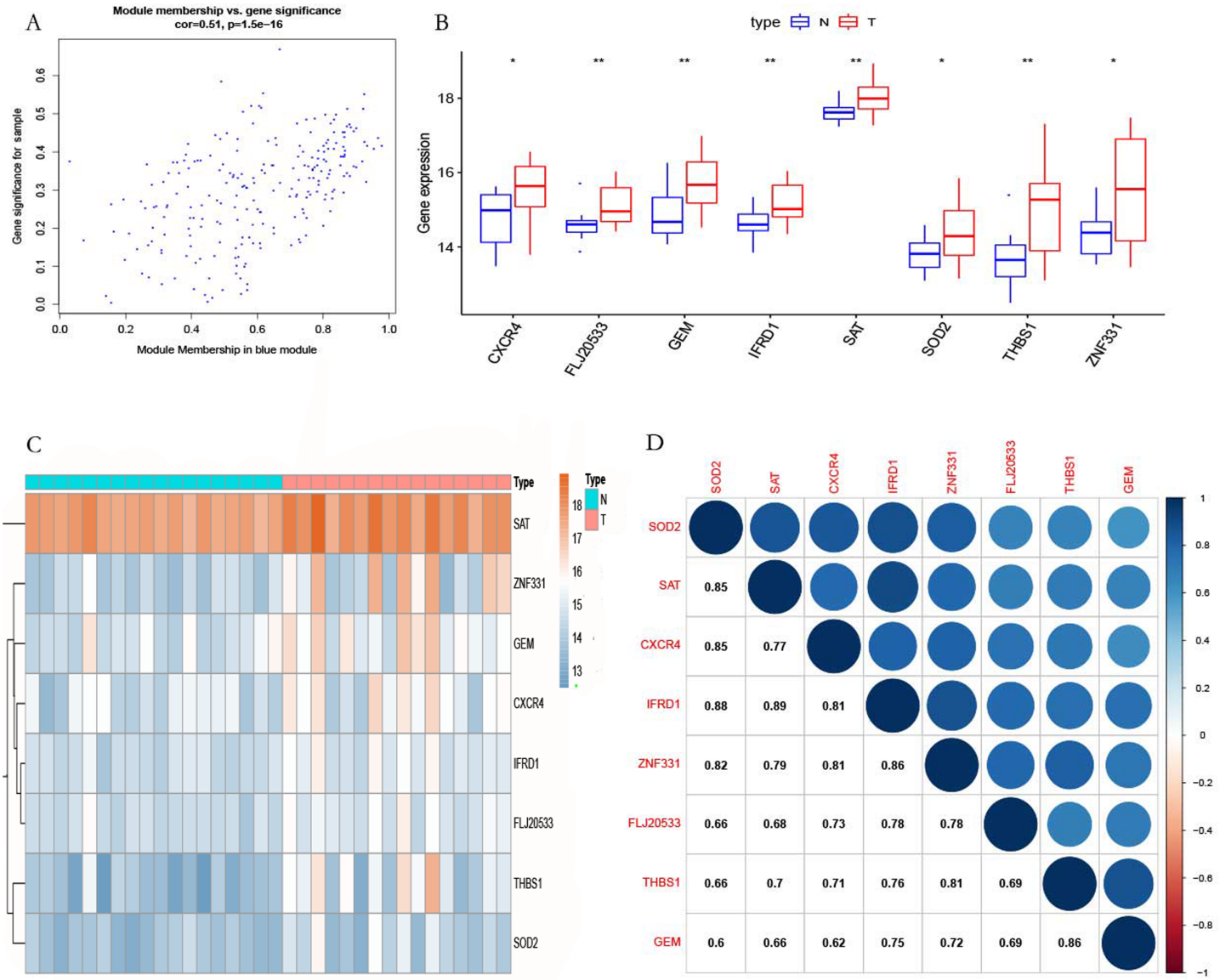

Figure 7 **Selected hub gene.** (A) The relationship between gene MM and GS. (B) Differential expression of the hub genes. (C) Heatmap of the hub genes in GSE12852. (D) Correlation analysis of the hub genes in GSE12852. Full-size DOI: 10.7717/peerj.9773/fig-7

related coefficient between the infiltration of different immune cells and hub genes. The results reveal that activated mast cells and neutrophils had a positive correlation with the hub genes, while resting mast cells had a negative correlation with the hub genes (Table 1).

DISCUSSION

Pelvic organ prolapse is caused by weakening of the supporting structures of the pelvic floor, resulting in the position of pelvic floor organs moving downward and the function becoming abnormal. POP seriously affects the quality of life of middle-aged and elderly women. In recent years, with the rapid development of gene sequencing and

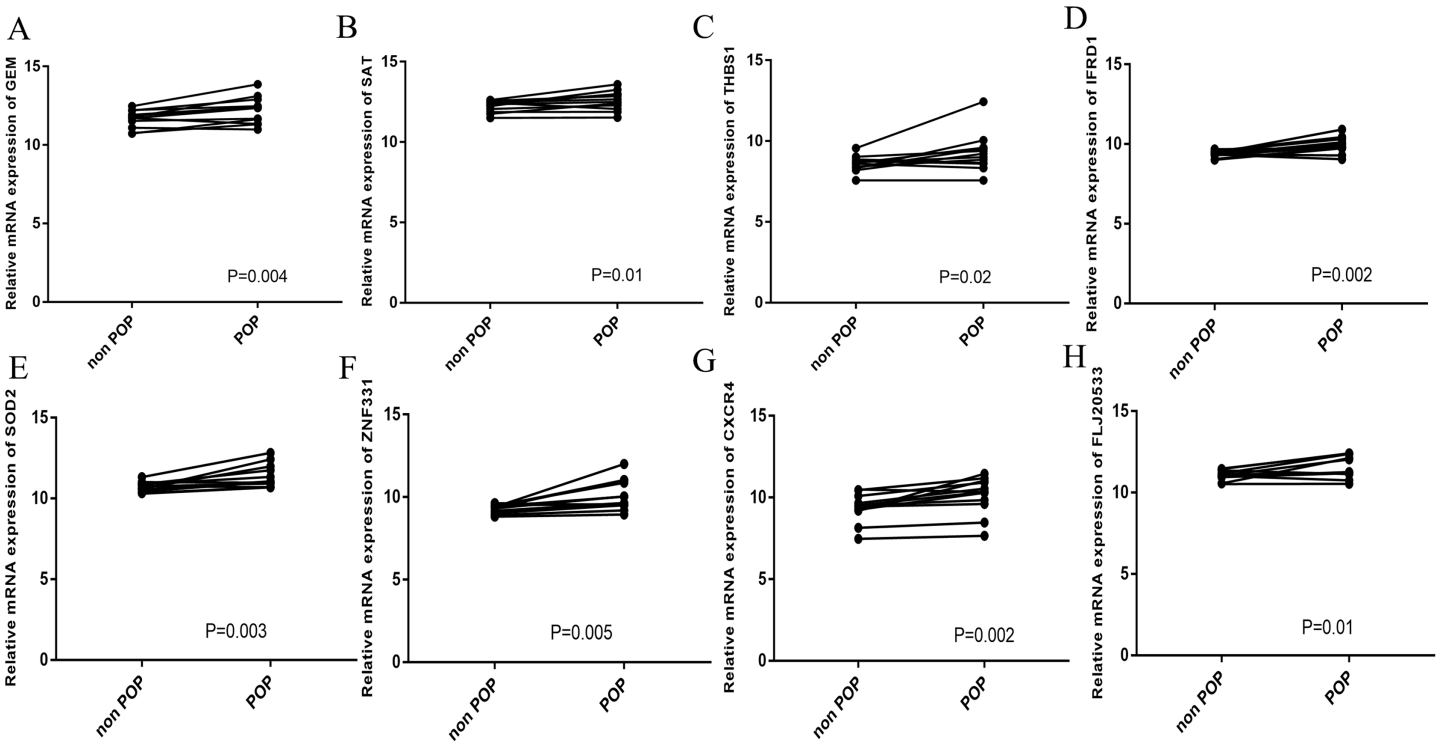

Figure 8 **Hub gene validation.** (A–H) RT-qPCR detection of the expression of hub genes in 12 pairs of POP and non-POP tissues.
Full-size DOI: 10.7717/peerj.9773/fig-8

bioinformatics technologies, further analysis and utilization of sequencing data have become possible. To explore the molecular mechanism related to the development of POP, eight hub genes (*ZNF331*, *THBS1*, *IFRD1*, *FLJ20533*, *CXCR4*, *GEM*, *SOD2*, and SAT) related to POP occurrence were screened out based on WGCNA and their biological functions were explored.

Thrombospondins (THBSs) are a group of glycoproteins that bind to collagen and tissue, participating in the interaction between cells and the extracellular matrix during the process of tissue development and repair. *THBS1* is the first member of the *THBS* gene family, which plays a significant role in many biological processes related to the occurrence and progression of cardiovascular diseases, such as angiogenesis, inflammation, and tissue remodeling (*Zhao, Isenberg & Popel, 2018*). In addition, *THBS1* can also affect tumor cell adhesion, invasion, migration, proliferation, apoptosis, and immune evasion (*Huang et al., 2017*). The overexpression of *THBS1* in POP tissues as compared with non-POP tissues has been predicted and verified (*Brizzolara, Killeen & Urschitz, 2009*), which is consistent with the results of our secondary analysis. *ZNF331* is located on chromosome 19q13, a recently cloned gene encoding a zinc-finger protein involved in thyroid tumorigenesis (*Babinger et al., 2007*). *ZNF331*, as a tumor suppressor gene, has also been reported to have low expression in colorectal cancer (*Wang et al., 2017*), esophageal cancer (*Jiang et al., 2015*), gastric cancer (*Yu et al., 2013*), and liver cancer (*Wang et al., 2013*), and its low expression is related to hypermethylation of its promoter region. However, the research on *ZNF331* in other diseases was rare. *Interferon-related*

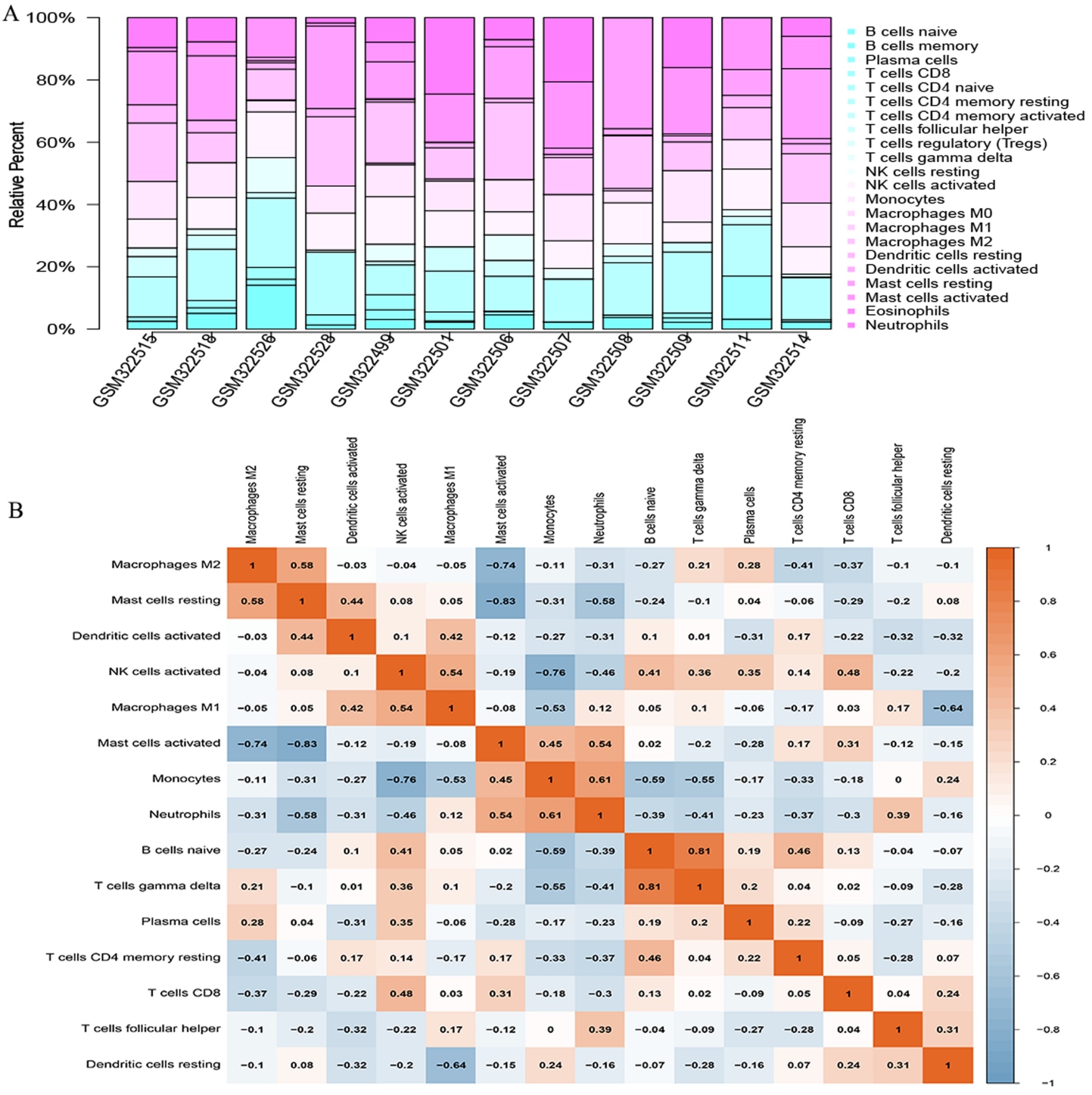

Figure 9 The landscape of immune cell infiltration in GSE12852 (CIBERSORT *p* value < 0.05). (A) Proportion of the 22 immune cell types in GSE12852. (B) Correlation matrix between the 22 immune cell types. Full-size DOI: 10.7717/peerj.9773/fig-9

developmental regulator 1 (*IFRD1*) is located on chromosome 7q22-q31 and acts a significant role in the development and differentiation of embryonic muscle cells (*Kraus, Haenig & Kispert, 2001*; *Lincoln, Alfieri & Yutzey, 2004*). *IFRD1* has been proved to be a

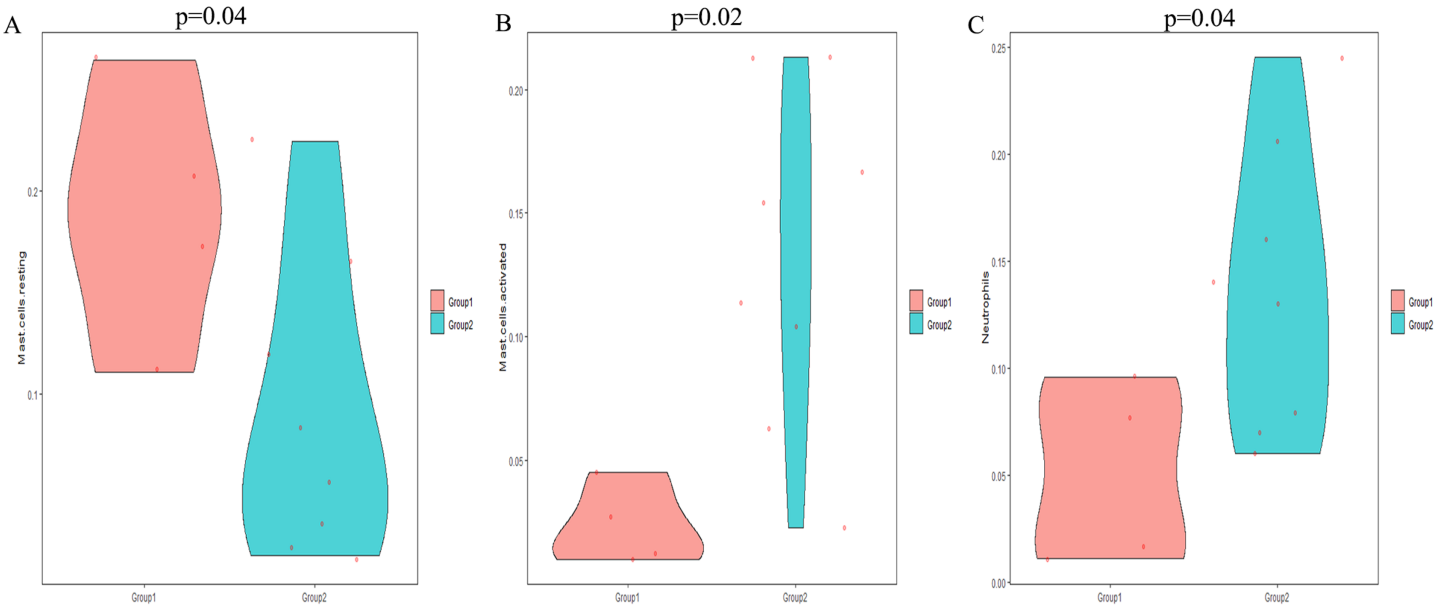

Figure 10 The differential immune cell infiltration between POP and non-POP tissues. (A) Resting mast cells; (B) activated mast cells; (C) neutrophils. Group 1: non-POP; Group 2: POP. Full-size DOI: 10.7717/peerj.9773/fig-10

Table 1 The correlation between hub genes and immune cell infiltration.

Gene	Immune cell	*P*	*R*
CXCR4	Mast cells activated	0.026025009	0.636596855
FLJ20533	Mast cells activated	0.037410947	0.604312579
GEM	Mast cells activated	0.00382779	0.763874376
IFRD1	Mast cells activated	0.010102021	0.707220887
SAT	Mast cells activated	0.026678483	0.634493564
SOD2	Mast cells activated	0.019559382	0.659816924
THBS1	Mast cells activated	0.023473376	0.645196019
ZNF331	Mast cells activated	0.005806179	0.741209161
GEM	Mast cells resting	0.044390877	−0.587895781
IFRD1	Mast cells resting	0.010475671	−0.704821204
SAT	Mast cells resting	0.029213165	−0.626671202
SOD2	Mast cells resting	0.002740399	−0.780472841
CXCR4	Neutrophils	0.002884121	0.778019124
FLJ20533	Neutrophils	0.009179588	0.713441726
GEM	Neutrophils	0.030016479	0.624294555
IFRD1	Neutrophils	0.001688177	0.802313109
SAT	Neutrophils	0.001387584	0.810472605
SOD2	Neutrophils	2.12E−04	0.872716498
THBS1	Neutrophils	0.014406502	0.682777143
ZNF331	Neutrophils	0.002414909	0.786415881

modified gene of cystic fibrosis lung disease, which can regulate the effector function of neutrophil (*Gu et al., 2009*). Transmembrane protein 70 (TMEM70), also named FLJ20533, is a mitochondrial membrane protein that acts a role in the biosynthesis of mitochondrial ATPase (*Hejzlarova et al., 2011*). At present, research related to TMEM70 mainly focuses on cardiomyopathy and pulmonary hypertension. CXCR4, also known as CD184, is a highly conserved receptor for the chemokine CXCL12 (*Kashyap et al., 2017*). CXCR4 belongs to the *G* protein-coupled receptor superfamily and is expressed in a cortical protein-dependent manner on the cell surface (*Teicher & Fricker, 2010*). CXCR4 has been reported to be overexpressed in a variety of tumor cells and is involved in tumor proliferation, invasion, metastasis, and worse prognosis (*Ottaiano et al., 2020*; *Wang et al., 2020a*; *Zhu et al., 2020*). GTP-binding protein overexpressed in skeletal muscle (GEM) is a GTPase originally identified in mitogen-stimulated *T* lymphocytes and v-Abl-transformed pre-*B* cells and is highly expressed in the spleen, thymus, and kidneys (*Cohen et al., 1994*; *Huang et al., 2014*). Mitochondrial superoxide dismutase (SOD2) is an antioxidant enzyme that reduces the damage caused by oxidative stress to protect mitochondria (*Koltai et al., 2018*). Spermidine/spermine N1-acetyltransferase (SAT) is the rate-limiting enzyme in polyamine catabolism and functions through the acetylation of spermidine and spermidine to affect cell growth, proliferation, and apoptosis (*Pegg, 2008*, *2016*). Despite a detailed literature review, we found no reports of the involvement *ZNF331*, *IFRD1*, *FLJ20533*, *CXCR4*, *GEM*, *SOD2*, or *SAT* in POP. To explore the expression of the selected hub genes in POP and non-POP tissues, differential analysis of the GSE12852 dataset was performed by RT-qPCR. The results indicate that the selected hub genes were overexpressed in POP tissues as compared with non-POP tissues, suggesting that the selected hub genes may be related to POP occurrence.

GO and KEGG functional enrichment analyses were performed to study the function of the hub genes using the "R" software. GO functional annotation showed that the hub genes were mainly participated in the immune response. KEGG enrichment analysis revealed that the hub genes participated in the regulation of immune-related pathways such as the IL-17 signaling pathway. IL-17 is a member of the inflammatory cytokine family and is mainly produced by Th17 cells. IL-17 signaling has been reported to be associated with immunopathology and autoimmune diseases (*Amatya, Garg & Gaffen, 2017*). Previous research has confirmed that the extracellular matrix components in connective tissue can control the physical strength of the pelvic floor (*Dietz, Jarvis & Vancaillie, 2002*). The immune system can maintain the homeostasis of POP tissues by adjusting extracellular matrix components (*Yu et al., 2010*); thus, it is reasonable to suggest that regulation of the immune system is closely related to the occurrence of POP.
At present, there is no direct evidence indicating that IL-17 is related to POP occurrence; however, we have reason to believe that the IL-17 signaling pathway plays a significant role in the development of POP given its role in immune regulation. In view of the close relationship between hub genes and immunity, we investigated immune cell infiltration in POP and non-POP tissues using the CIBERSORT algorithm. We found a higher infiltration of activated mast cells and neutrophils in POP tissues than in non-POP tissues,

while infiltration of resting mast cells was lower in POP tissues. Activated mast cells and neutrophils had a positive correlation with the hub genes, while resting mast cells had a negative correlation. According to the results, it is reasonable to suggest that the hub genes may be related to the development of POP by regulating the levels of activated/resting mast cells and neutrophils. Mast cells are important antigen-presenting cells that can release histamine and cytokines through degranulation and act a significant role in the occurrence and development of various inflammatory diseases (*Grabauskas et al., 2020*; *Novruzov, 2008*; *Sajay-Asbaghi et al., 2020*). Very recently, THBS1 was demonstrated to promote the inflammatory response of mast cells in chronic idiopathic urticaria and the permeability of human dermal microvascular endothelial cells by regulating the TGF-β/SMAD pathway, the effects of which can be inhibited by miR-194 (*Qu, Yang & Liu, 2020*). Several studies have shown that CXCR4 can promote mast cell chemotaxis to inflammatory sites (*Limón-Flores et al., 2009*; *Lv et al., 2019*; *Patadia et al., 2010*), and IFRD1 may involve in neutrophilic inflammation in cystic fibrosis (*Blanchard et al., 2011*; *Gu et al., 2009*; *Hector et al., 2013*). According to the current literature, there is no direct evidence to prove the accuracy of our prediction results; however, the relationship between the hub genes and infiltration of different immune cells suggests they are correct.

Some limitations of this research need to be discussed. Firstly, the research remained at the prediction stage and there is insufficient experimental evidence to verify our prediction results. In the future, verification in vitro and in vivo should strengthen our observations. Secondly, the sample size for this study was not large enough due to the limited datasets in the database, which may have caused some bias. Thirdly, the samples of our research were coming from the ligamentum. The ligamentum are full of fibroblasts and it is not sure that they capture many white blood cells. We could not guarantee the accuracy of the CIBERSORT algorithms completely due to the blood specificity of the algorithms.

CONCLUSIONS

Our research identified eight hub genes and three immune cell types that may be related to POP occurrence. These hub genes may participate in the pathogenesis of POP by regulating the immune environment, giving them certain diagnostic and therapeutic value in POP.

ACKNOWLEDGEMENTS

We thank the authors who provided the GEO public datasets.

ADDITIONAL INFORMATION AND DECLARATIONS

Funding

This article was funded by Shengjing Hospital of China Medical University. The funders had no role in study design, data collection and analysis, decision to publish, or preparation of the manuscript.

Grant Disclosures

The following grant information was disclosed by the authors:
Shengjing Hospital of China Medical University.

Competing Interests

The authors declare that they have no competing interests.

Author Contributions

- Ying Zhao conceived and designed the experiments, performed the experiments, analyzed the data, prepared figures and/or tables, authored or reviewed drafts of the paper, and approved the final draft.
- Zhijun Xia conceived and designed the experiments, analyzed the data, prepared figures and/or tables, authored or reviewed drafts of the paper, and approved the final draft.
- Te Lin performed the experiments, analyzed the data, authored or reviewed drafts of the paper, and approved the final draft.
- Yitong Yin performed the experiments, analyzed the data, prepared figures and/or tables, authored or reviewed drafts of the paper, and approved the final draft.

Human Ethics

The following information was supplied relating to ethical approvals (i.e., approving body and any reference numbers):

The Ethics Committee of Shengjing Hospital of China Medical University approved the study protocol in accordance with the guidelines of the Declaration of Helsinki (No. 2018Ps68K), in accordance with the guidelines of the Helsinki Declaration.

Data Availability

The following information was supplied regarding data availability:

The sequence is available at NCBI GEO (GSE12852) and the PCR data are available as a Supplemental File.

Supplemental Information

Supplemental information for this article can be found online at http://dx.doi.org/10.7717/peerj.9773#supplemental-information.

REFERENCES

Amatya N, Garg AV, Gaffen SL. 2017. IL-17 signaling: the yin and the yang. *Trends in Immunology* **38(5)**:310–322 DOI 10.1016/j.it.2017.01.006.

Babinger P, Volkl R, Cakstina I, Maftei A, Schmitt R. 2007. Maintenance DNA methyltransferase (Met1) and silencing of CpG-methylated foreign DNA in *Volvox carteri*. *Plant Molecular Biology* **63(3)**:325–336 DOI 10.1007/s11103-006-9091-1.

Blanchard E, Marie S, Riffault L, Bonora M, Tabary O, Clement A, Jacquot J. 2011. Reduced expression of Tis7/IFRD1 protein in murine and human cystic fibrosis airway epithelial cell models homozygous for the F508del-CFTR mutation. *Biochemical and Biophysical Research Communications* **411(3)**:471–476 DOI 10.1016/j.bbrc.2011.06.104.

Brizzolara SS, Killeen J, Urschitz J. 2009. Gene expression profile in pelvic organ prolapse. *Molecular Human Reproduction* **15(1)**:59–67 DOI 10.1093/molehr/gan074.

Cai W, Li H, Zhang Y, Han G. 2020. Identification of key biomarkers and immune infiltration in the synovial tissue of osteoarthritis by bioinformatics analysis. *PeerJ* **8(Suppl. 1)**:e8390 DOI 10.7717/peerj.8390.

Chen B, Khodadoust MS, Liu CL, Newman AM, Alizadeh AA. 2018a. Profiling tumor infiltrating immune cells with CIBERSORT. *Methods in Molecular Biology* **1711**:243–259 DOI 10.1007/978-1-4939-7493-1_12.

Chen Y, Bi F, An Y, Yang Q. 2018b. Coexpression network analysis identified Kruppel-like factor 6 (KLF6) association with chemosensitivity in ovarian cancer. *Journal of Cellular Biochemistry* **120(2)**:2607–2615 DOI 10.1002/jcb.27567.

Cohen L, Mohr R, Chen YY, Huang M, Kato R, Dorin D, Tamanoi F, Goga A, Afar D, Rosenberg N. 1994. Transcriptional activation of a ras-like gene (kir) by oncogenic tyrosine kinases. *Proceedings of the National Academy of Sciences* **91(26)**:12448–12452 DOI 10.1073/pnas.91.26.12448.

Dietz HP, Jarvis SK, Vancaillie TG. 2002. The assessment of levator muscle strength: a validation of three ultrasound techniques. *International Urogynecology Journal* **13(3)**:156–159 DOI 10.1007/s192-002-8346-5.

Friedman T, Eslick GD, Dietz HP. 2018. Risk factors for prolapse recurrence: systematic review and meta-analysis. *International Urogynecology Journal* **29(1)**:13–21 DOI 10.1007/s00192-017-3475-4.

Grabauskas G, Wu X, Gao J, Li J-Y, Turgeon DK, Owyang C. 2020. Prostaglandin E2, produced by mast cells in colon tissues from patients with irritable bowel syndrome, contributes to visceral hypersensitivity in mice. *Gastroenterology* **158(8)**:2195–2207 DOI 10.1053/j.gastro.2020.02.022.

Gu Y, Harley IT, Henderson LB, Aronow BJ, Vietor I, Huber LA, Harley JB, Kilpatrick JR, Langefeld CD, Williams AH, Jegga AG, Chen J, Wills-Karp M, Arshad SH, Ewart SL, Thio CL, Flick LM, Filippi MD, Grimes HL, Drumm ML, Cutting GR, Knowles MR, Karp CL. 2009. Identification of IFRD1 as a modifier gene for cystic fibrosis lung disease. *Nature* **458(7241)**:1039–1042 DOI 10.1038/nature07811.

Haya N, Feiner B, Baessler K, Christmann-Schmid C, Maher C. 2018. Perioperative interventions in pelvic organ prolapse surgery. *Cochrane Database of Systematic Reviews* **8(1)**:Cd013105 DOI 10.1002/14651858.Cd013105.

Hector A, Kormann M, Kammermeier J, Burdi S, Marcos V, Rieber N, Mays L, Illig T, Klopp N, Falkenstein F, Kappler M, Riethmueller J, Graepler-Mainka U, Stern M, Eickmeier O, Serve F, Zielen S, Döring G, Griese M, Hartl D. 2013. Expression and regulation of interferon-related development regulator-1 in cystic fibrosis neutrophils. *American Journal of Respiratory Cell and Molecular Biology* **48(1)**:71–77 DOI 10.1165/rcmb.2012-0061OC.

Hejzlarova K, Tesarova M, Vrbacka-Cizkova A, Vrbacky M, Hartmannova H, Kaplanova V, Noskova L, Kratochvilova H, Buzkova J, Havlickova V, Zeman J, Kmoch S, Houstek J. 2011. Expression and processing of the TMEM70 protein. *Biochimica et Biophysica Acta* **1807(1)**:144–149 DOI 10.1016/j.bbabio.2010.10.005.

Hendrix SL, Clark A, Nygaard I, Aragaki A, Barnabei V, McTiernan A. 2002. Pelvic organ prolapse in the women's health initiative: gravity and gravidity. *American Journal of Obstetrics and Gynecology* **186(6)**:1160–1166 DOI 10.1067/mob.2002.123819.

Huang T, Sun L, Yuan X, Qiu H. 2017. Thrombospondin-1 is a multifaceted player in tumor progression. *Oncotarget* **8(48)**:84546–84558 DOI 10.18632/oncotarget.19165.

Huang X, Cong X, Yang D, Ji L, Liu Y, Cui X, Cai J, He S, Zhu C, Ni R, Zhang Y. 2014. Identification of gem as a new candidate prognostic marker in hepatocellular carcinoma. *Pathology—Research and Practice* **210(11)**:719–725 DOI 10.1016/j.prp.2014.07.001.

Jiang S, Linghu E, Zhan Q, Han W, Guo M. 2015. Methylation of ZNF331 promotes cell invasion and migration in human esophageal cancer. *Current Protein & Peptide Science* **16(4)**:322–328 DOI 10.2174/1389203716041504291552 55.

Kashyap MK, Amaya-Chanaga CI, Kumar D, Simmons B, Huser N, Gu Y, Hallin M, Lindquist K, Yafawi R, Choi MY, Amine A-A, Rassenti LZ, Zhang C, Liu S-H, Smeal T, Fantin VR, Kipps TJ, Pernasetti F, Castro JE. 2017. Targeting the CXCR4 pathway using a novel anti-CXCR4 IgG1 antibody (PF-06747143) in chronic lymphocytic leukemia. *Journal of Hematology & Oncology* **10(1)**:112 DOI 10.1186/s13045-017-0435-x.

Koltai E, Bori Z, Osvath P, Ihasz F, Peter S, Toth G, Degens H, Rittweger J, Boldogh I, Radak Z. 2018. Master athletes have higher miR-7, SIRT3 and SOD2 expression in skeletal muscle than age-matched sedentary controls. *Redox Biology* **19**:46–51 DOI 10.1016/j.redox.2018.07.022.

Kraus F, Haenig B, Kispert A. 2001. Cloning and expression analysis of the mouse T-box gene tbx20. *Mechanisms of Development* **100(1)**:87–91 DOI 10.1016/S0925-4773(00)00499-8.

Limón-Flores AY, Chacón-Salinas R, Ramos G, Ullrich SE. 2009. Mast cells mediate the immune suppression induced by dermal exposure to JP-8 jet fuel. *Toxicological Sciences* **112(1)**:144–152 DOI 10.1093/toxsci/kfp181.

Lin J, Yu M, Xu X, Wang Y, Xing H, An J, Yang J, Tang C, Sun D, Zhu Y. 2020. Identification of biomarkers related to CD8(+) T cell infiltration with gene co-expression network in clear cell renal cell carcinoma. *Aging* **12(4)**:3694–3712 DOI 10.18632/aging.102841.

Lincoln J, Alfieri CM, Yutzey KE. 2004. Development of heart valve leaflets and supporting apparatus in chicken and mouse embryos. *Developmental Dynamics* **230(2)**:239–250 DOI 10.1002/dvdy.20051.

Liu R, Hu R, Zeng Y, Zhang W, Zhou H-H. 2020. Tumour immune cell infiltration and survival after platinum-based chemotherapy in high-grade serous ovarian cancer subtypes: a gene expression-based computational study. *EBioMedicine* **51**:102602 DOI 10.1016/j.ebiom.2019.102602.

Lv Y, Zhao Y, Wang X, Chen N, Mao F, Teng Y, Wang T, Peng L, Zhang J, Cheng P, Liu Y, Kong H, Chen W, Hao C, Han B, Ma Q, Zou Q, Chen J, Zhuang Y. 2019. Increased intratumoral mast cells foster immune suppression and gastric cancer progression through TNF-α-PD-L1 pathway. *Journal for Immunotherapy of Cancer* **7(1)**:54 DOI 10.1186/s40425-019-0530-3.

Novruzov RM. 2008. Hemomicrocirculation channel and mastocyte population in outer oblique aponeurosis stomach muscles and uterus ligament in women with small pelvic organ prolapses. *Georgian Medical News* **164**:69–72.

Nygaard IE, Shaw JM, Bardsley T, Egger MJ. 2014. Lifetime physical activity and pelvic organ prolapse in middle-aged women. *American Journal of Obstetrics and Gynecology* **210(5)**:477.e1–477.e12 DOI 10.1016/j.ajog.2014.01.035.

Ottaiano A, Scala S, Normanno N, Botti G, Tatangelo F, Di Mauro A, Capozzi M, Facchini S, Tafuto S, Nasti G. 2020. Prognostic and predictive role of CXC chemokine receptor 4 in metastatic colorectal cancer patients. [Epub ahead of print 23 January 2020]. *Applied Immunohistochemistry & Molecular Morphology* DOI 10.1097/PAI.0000000000000828.

Patadia M, Dixon J, Conley D, Chandra R, Peters A, Suh LA, Kato A, Carter R, Harris K, Grammer L, Kern R, Schleimer R. 2010. Evaluation of the presence of B-cell attractant

chemokines in chronic rhinosinusitis. *American Journal of Rhinology & Allergy* **24(1)**:11–16 DOI 10.2500/ajra.2010.24.3386.

Pegg AE. 2008. Spermidine/spermine-N(1)-acetyltransferase: a key metabolic regulator. *American Journal of Physiology* **294(6)**:E995–E1010 DOI 10.1152/ajpendo.90217.2008.

Pegg AE. 2016. Functions of polyamines in mammals. *Journal of Biological Chemistry* **291(29)**:14904–14912 DOI 10.1074/jbc.R116.731661.

Qu S, Yang L, Liu Z. 2020. MicroRNA-194 reduces inflammatory response and human dermal microvascular endothelial cells permeability through suppression of TGF-β/SMAD pathway by inhibiting THBS1 in chronic idiopathic urticaria. *Journal of Cellular Biochemistry* **121(1)**:111–124 DOI 10.1002/jcb.28941.

Sajay-Asbaghi M, Sadeghi-Shabestrai M, Monfaredan A, Seyfizadeh N, Razavi A, Kazemi T. 2020. Promoter region single nucleotide polymorphism of siglec-8 gene associates with susceptibility to allergic asthma. *Personalized Medicine* **17(3)**:195–201 DOI 10.2217/pme-2018-0080.

Teicher BA, Fricker SP. 2010. CXCL12 (SDF-1)/CXCR4 pathway in cancer. *Clinical Cancer Research* **16(11)**:2927–2931 DOI 10.1158/1078-0432.CCR-09-2329.

Türei D, Korcsmáros T, Saez-Rodriguez J. 2016. OmniPath: guidelines and gateway for literature-curated signaling pathway resources. *Nature Methods* **13(12)**:966–967 DOI 10.1038/nmeth.4077.

Wang D, Wang X, Si M, Yang J, Sun S, Wu H, Cui S, Qu X, Yu X. 2020a. Exosome-encapsulated miRNAs contribute to CXCL12/CXCR4-induced liver metastasis of colorectal cancer by enhancing M2 polarization of macrophages. *Cancer Letters* **474**:36–52 DOI 10.1016/j.canlet.2020.01.005.

Wang H, Chen G, Wang H, Liu C. 2013. RITA inhibits growth of human hepatocellular carcinoma through induction of apoptosis. *Oncology Research* **20(10)**:437–445 DOI 10.3727/096504013X13685487925059.

Wang M, Wang J, Liu J, Zhu L, Ma H, Zou J, Wu W, Wang K. 2020b. Systematic prediction of key genes for ovarian cancer by co-expression network analysis. *Journal of Cellular and Molecular Medicine* **24(11)**:6298–6307 DOI 10.1111/jcmm.15271.

Wang Y, He T, Herman JG, Linghu E, Yang Y, Fuks F, Zhou F, Song L, Guo M. 2017. Methylation of ZNF331 is an independent prognostic marker of colorectal cancer and promotes colorectal cancer growth. *Clinical Epigenetics* **9(1)**:115 DOI 10.1186/s13148-017-0417-4.

Wu JM, Hundley AF, Fulton RG, Myers ER. 2009. Forecasting the prevalence of pelvic floor disorders in U.S. women: 2010 to 2050. *Obstetrics & Gynecology* **114(6)**:1278–1283 DOI 10.1097/AOG.0b013e3181c2ce96.

Yu J, Liang QY, Wang J, Cheng Y, Wang S, Poon TC, Go MY, Tao Q, Chang Z, Sung JJ. 2013. Zinc-finger protein 331, a novel putative tumor suppressor, suppresses growth and invasiveness of gastric cancer. *Oncogene* **32(3)**:307–317 DOI 10.1038/onc.2012.54.

Yu Q, Vazquez R, Zabadi S, Watson RR, Larson DF. 2010. T-lymphocytes mediate left ventricular fibrillar collagen cross-linking and diastolic dysfunction in mice. *Matrix Biology* **29(6)**:511–518 DOI 10.1016/j.matbio.2010.06.003.

Zhang B, Wang Q, Fu C, Jiang C, Ma S. 2019. Exploration of the immune-related signature and immune infiltration analysis for breast ductal and lobular carcinoma. *Annals of Translational Medicine* **7(23)**:730 DOI 10.21037/atm.2019.11.117.

Zhao C, Isenberg JS, Popel AS. 2018. Human expression patterns: qualitative and quantitative analysis of thrombospondin-1 under physiological and pathological conditions. *Journal of Cellular and Molecular Medicine* **22(4)**:2086–2097 DOI 10.1111/jcmm.13565.

Zhou Z, Cheng Y, Jiang Y, Liu S, Zhang M, Liu J, Zhao Q. 2018. Ten hub genes associated with progression and prognosis of pancreatic carcinoma identified by co-expression analysis. *International Journal of Biological Sciences* **14(2)**:124–136 DOI 10.7150/ijbs.22619.

Zhu Q, Luo R, Gu J, Hou Y, Chen Z, Xu F, Wang L, Mao W, Lu C, Ge D. 2020. High CXCR4 expression predicts a poor prognosis in resected lung Adenosquamous carcinoma. *Journal of Cancer* **11(4)**:810–818 DOI 10.7150/jca.36498.